Available online at www.sciencedirect.com

ScienceDirect

Energy Procedia 4 (2011) 2090–2095

Energy Procedia

www.elsevier.com/locate/procedia

GHGT-10

Modeling, synthesis and characterization of zinc containing carbonic anhydrase active site mimics

J. H. Satcher, Jr., S.E. Baker, H. J. Kulik, C. A. Valdez, R. L. Krueger, F. C. Lightstone, R. D. Aines

Physical and Life Sciences Directorate, Lawrence Livermore National Laboratory

Abstract

Two structurally similar carbonic anhydrase active site mimics are explored computationally and experimentally in order to gain insight into the impact of subtle differences in scaffold structure on CO_2 hydration rates.

Keywords: post combustion, carbon capture, advanced solvents, enzyme mimics

Introduction

Carbonic anhydrases are metalloproteins that reversibly catalyze the hydration and dehydration of CO_2 at ambient temperature and physiological pH. Carbonic anhydrase facilitates extremely fast CO_2 hydration rates, which are typically limited only by the diffusion rate of CO_2 to the active site. Therefore, carbonic anhydrase might be an ideal catalyst for enhancing industrial carbon capture. Unfortunately, the protein is not likely to survive the temperature and solvent conditions required. Current industrial carbon capture is facilitated by amine-based solvents which are used to increase capacity and the rate of CO_2 absorption. However, these basic amine solvents require significant energy to release the captured carbon dioxide during the regeneration process. Small molecule mimics of the carbonic anhydrase active site [1-4] are likely sufficiently stable to facilitate enhanced CO_2 hydration at near neutral pH, with a concomitant reduction in the energy penalty for regeneration, therefore have the potential to dramatically improve the post-combustion capture of carbon dioxide.

The active site of carbonic anhydrase consists of Zn^{2+} coordinated by three histidine imidazole groups and either a water molecule or hydroxyl group, depending on pH. The generally accepted mechanism of CO_2 hydration by carbonic anhydrase involves the nucleophilic attack by the Zn-hydroxyl group on the dissolved CO_2 molecule. Therefore, the pKa of the water coordinated to the Zn, and by extension the Zn coordination environment and geometry which contribute to this pKa value, are critical to the performance of the catalyst. In order to enhance our understanding of the geometric and energetic factors that influence CO_2 hydration catalyst activity, here we explore two carbonic anhydrase active site mimics: cyclen-Zn^{2+} and cyclam-Zn^{2+}. Cyclen-Zn^{2+} is a cyclic tetra-aza complex

doi:10.1016/j.egypro.2011.02.092

which is one of the most active carbonic anhydrase mimics known.[2] Cyclam-Zn^{2+} is a similar cyclic amine complex but contains two additional methylene groups (Scheme 1). The cyclen and cyclam ligands have comparably high Zn^{2+} binding constants. [5] High Zn^{2+} binding affinity has been conjectured to contribute to the high activity of cyclen-Zn^{2+}, but to our knowledge the CO_2 hydration activity for cyclam-Zn^{2+} has not been reported. However, the pKa values for the coordinated water are 8.02 and 9.77 for cyclen and cyclam-Zn^{2+}, respectively, indicating dramatically different Zn^{2+} coordination environments.[5] Higher pKas of coordinated water have been correlated with higher catalyst activities.[2] Therefore, the computational and experimental comparison between these two similar catalysts will shed light on how slight changes in active site geometry influence catalyst activity.

Methods

Simulations

Density functional theory simulations were carried out using the Perdew-Burke-Ernzerhof generalized gradient approximation exchange-correlation functional. These calculations were completed in a plane-wave, periodic boundary condition formalism with ultrasoft pseudopotentials to represent the core electrons of the atoms. The pseudopotentials for Co and Zn include both *3d* and *4s* states in the valence. The wavefunction and charge density cutoff are 30 and 300 Ry, respectively. All calculations were completed using a supercell with at least 8 Å separation between neighboring molecules to prevent periodic image effects. All intermediates are relaxed fully, unless otherwise specified. Transition states are determined using the nudged elastic band method with climbing images implemented. All systems with neutral axial ligands had a net +2 charge overall, while the systems with negatively charged axial ligands had a net charge of +1.

Synthesis of Cyclen and Cyclam-based Zinc(II) catalysts

Reagent grade chemicals were used as received from VWR and Aldrich. NMR spectra were determined using solutions of the catalysts in D_2O or DMSO-$_{d6}$. Mass spectra (MS) were obtained using a Quadrupole Mass Analyzer and Atmospheric Pressure Chemical Ionization ($APCI^+$) in the positive ion mode.

The synthesis of the catalysts involves the treatment of the aza-macrocyclic scaffold with the perchlorate salt of the metal, and heating of the mixture at 60 °C (Scheme 1).[6-8] After cooling the mixture, filtering of the solid is accomplished using vacuum filtration, and recrystallization of the catalyst is achieved in Ethanol.

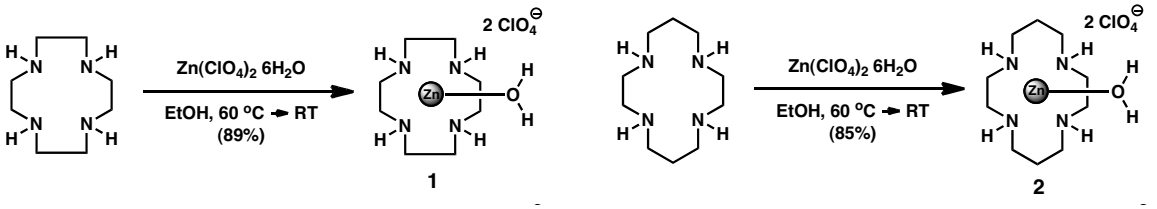

Scheme 1. Preparation of catalysts described herein.

Cyclen-Zn(II) perchlorate salt (**1**) – and Cyclam-Zn(II) perchlorate salt (**2**) were dissolved in ethanol. The colorless solution was heated to 60 °C, and at this temperature while stirring, a solution of $Zn(ClO_4)_2$ $6H_2O$ in EtOH was added *via* addition funnel dropwise to it over 10 minutes. The resulting white suspension was stirred at 60 °C for 30 minutes and then at ambient temperature for 2 hours. The white solid was isolated *via* vacuum filtration and washed with EtOH. The white solid was then taken up in EtOH (30 mL) and heated until it was fully dissolved in the solution, then placed at 6°C overnight for crystallization to take place. The white solid obtained after recrystallization was that of the cyclen-Zn(II) perchlorate complex (9.38 g, 89%) or cyclam-Zn(II) perchlorate complex (4.10 g, 85%).

Kinetic Measurements

All buffers and indicators were used as purchased from Sigma Aldrich. The kinetic measurements were performed using an Applied Photophysics stopped-flow attachment in conjunction with a uv/vis spectrophotometer, using the "change in pH indicator technique." Using this technique, a buffer/indicator pair is chosen with similar pKa values, so that the rate of change in optical absorbance of the pH indicator can be directly related to rate of carbonic acid formation, and thus catalyst activity. The experimental methods and data treatment have been described in detail elsewhere.[3,9] Here, we measured catalyst activities at pH 7.5 using HEPES buffer and phenol red pH indicator, pH 9.0,using AMPSO buffer and Thymol Blue pH indicator, and pH 9.8 using CHES buffer and Thymol Blue indicator.

Results and Discussion

We are interested in the impact that subtle differences in scaffold structure can have on relative energetic and thus CO_2 hydration rates. We thus began by comparing the differences of cyclen and cyclam structures, which differ by the latter having an additional two carbons in the ring structure. These differences in the cyclam confer greater flexibility, which we will later discuss in greater detail. Alignment of relaxed cyclen and cyclam structures shows that overall the resting state of the metal-scaffold complex has a reduced displacement of the metal from the nitrogen plane for the cyclam than the cyclen (Figure 1a). However, the apparent M-N distances are somewhat similar, with the cyclam being only slightly shorter (see Table 2).

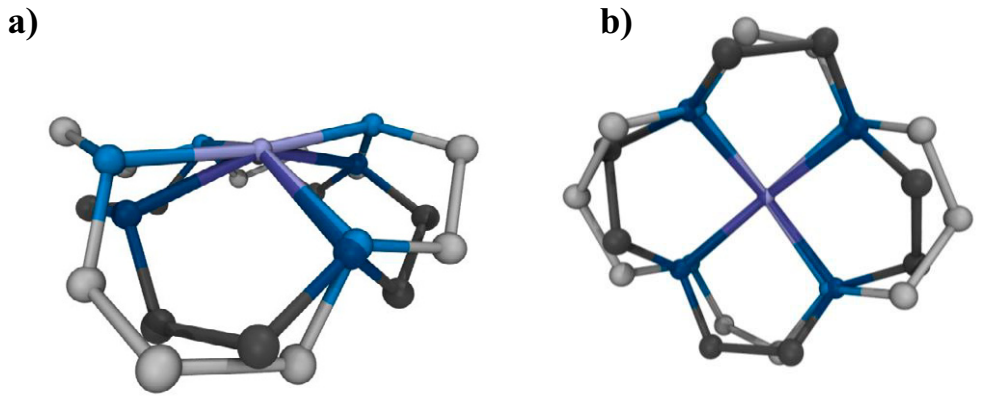

Figure 1. Alignment of the molecule cyclen-Zn (dark) with cyclam-Zn(light) with two perspectives shown (atom colors are Zn: purple, N: blue, C: grey). In both cases, the conformers correspond to the hydrogens on each nitrogen (not shown) being aligned on one side of the molecule. a) The cyclam-Zn induces a flatter Zn-N coordination environment, while the cyclen-Zn is more domed. b) The two structures exhibit comparable Zn-N distances.

Table 1. Comparison of bond lengths (in Å) and dihedral angles (in °) for the Zn^{2+} cyclen and cyclam structures. In the case of the cyclam, two conformers are reported, half up and half down hydrogens (H) and all up hydrogens (A).

	Cyclen	Cyclam(H)	Cyclam(A)
$r(\text{M-N})_{avg}$	2.23	2.17	2.20
r(M-OH)	1.85	1.91	1.88
Dih(M-N)	29	17	33

Computational investigations were carried out on both cyclen and cyclam scaffolds with Zn^{2+} metal centers. In the case of cyclam, several conformers are close in energy, but we choose two conformers as limiting cases for this preliminary investigation. We distinguish the two conformers by the orientation of the hydrogens that are coordinated to the metal-coordinating nitrogens. In the first conformer, there are two hydrogens that are aligned

with one side of the molecule and there are two hydrogens that are aligned with the other side (referred to as the H conformer for half and half). In the other conformer, all nitrogen-coordinating hydrogens are aligned to one face of the molecule (referred to as the A conformer for all on one side). The main difference between these two conformers is that the staggering of the hydrogens in the H conformer induces a relatively flat scaffold and coordinating environment around the metal, while the A conformer exhibits greater curvature (Figure 2). Alignment of the two conformers shows that the Zn^{2+} center sits in the plane of the nitrogens for both uncoordinated A and H species, despite differences in curvature of the two scaffolds. Doming occurs when an axial ligand is present in both conformers, but the amount that Zn is displaced from the plane is greatly enhanced in the A structure over the H structure. In addition to structural differences, we are interested in isolating the energetic differences of the reaction pathway for differing conformers in order to work towards an understanding of whether the relative populations of these conformers and barriers to interconversion play a role in reaction rates.

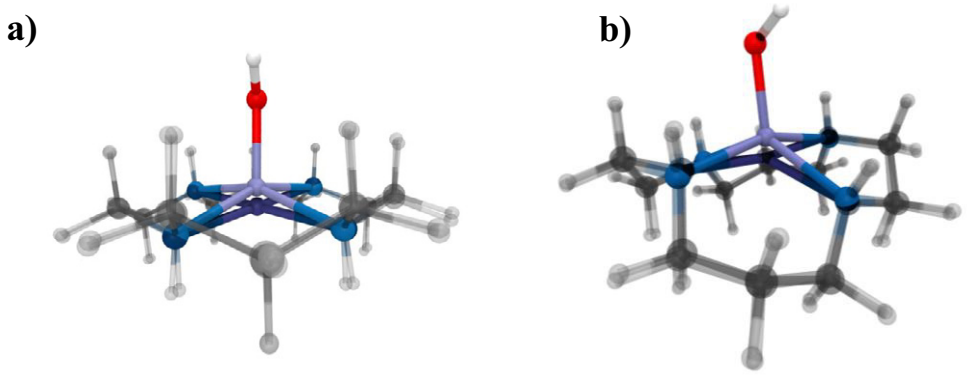

Figure 2. Alignment of cyclam-Zn-OH (light) with cyclam-Zn (dark) in two conformers (atom colors are Zn: purple, N: blue, C: grey, O: red, H: white). The two conformers shown are a) two H up and two H down and b) all H up. In both cases, the displacement of Zn from the nitrogen plane is significant when an axial hydroxyl is present. The carbon atoms are represented translucently for clarity.

We compare the activation energy (ΔE_a) of the step to form bicarbonate from CO_2 and an axial hydroxyl ligand and report it for the structures in Table 2. The energetics suggest that single conformers of the cyclam catalyze the reaction more slowly than the cyclen structure does. Additionally, we do not take into account any effect of conformer exchange or equilibrium that might further reduce the reactivity of the cyclam. Comparison of the net reaction energetics shows that this reaction step is favorable for all mimic configurations considered. Product release, as defined as the exchange of a carbonic acid molecule with a water molecule, also favorable for both cyclen and cyclam ligands. Thus we predict based on structural and energetic calculations that cyclen will have greater catalytic activity based on the more rigid Zn coordinating environment and the lower activation energy required for bicarbonate formation.

Table 2. Comparison of energetics (in kcal/mol) for the Zn^{2+} cyclen and cyclam structures. In the case of the cyclam, two conformers are reported, half up and half down hydrogens (H) and all up hydrogens (A).

	Zn^{2+}		
	Cyclen	Cyclam(H)	Cyclam(A)
ΔE_a	5.6	6.7	7.6
ΔE_{rxn}	-11	-10	-12
Prod. Rel.	-5.6	-2.2	-4.3

In order to corroborate our computational results, we compared the rates of CO_2 hydration by cyclen-Zn^{2+} and cyclam-Zn^{2+} at varied pH using the "change in pH indicator" technique, as described in the Methods section. Figure 3 shows the initial catalyst velocity for both cyclen and cyclam as a function of increasing catalyst concentration. Dotted lines represent weighted linear fits to the data, which were used to calculate the rate constants shown in Table 3, as described previously. [2]

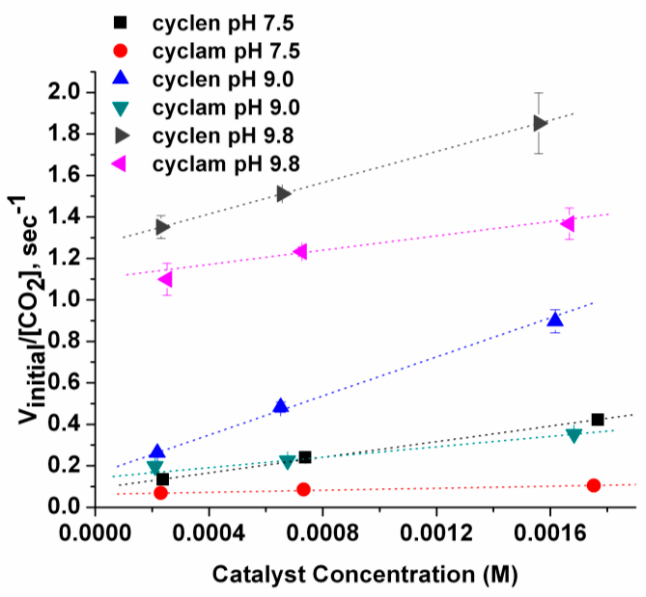

Figure 3. Initial rates of CO_2 hydration by cyclen and cyclam -Zn^{2+} as a function of catalyst concentration at pH 7.5, 9.0, and 9.8.

Table 3. Observed second order rate constants derived from the slopes of the lines in Figure 3.

	Cyclen $(k^h_{cat})_{obs}$, $M^{-1}s^{-1}$	**Cyclam** $(k^h_{cat})_{obs}$, $M^{-1}s^{-1}$
pH 7.5	188 ± 3	24 ± 3
pH 9.0	471 ± 33	126 ± 4
pH 9.8	388 ± 113	172 ± 73

At the pH values studied, both catalysts generally displayed higher activities at higher pH values, consistent with increasing availability of Zn-OH sites for the nucleophilic attack of dissolved CO_2 (Table 3). However, cyclen-Zn^{2+} was found to have ~ 8 times greater observed rate constant than cyclam-Zn^{2+} at pH 7.5, ~ 4 times greater at pH 9.0, and ~2 times greater at pH 9.8. The narrowing activity gap between cyclam and cyclen at higher pH values is likely due to the higher pKa of cyclam-Zn-OH_2 (9.77), compared with the pKa of cyclen-Zn-OH_2, (8.02).[5] As shown in Figure 3, increasing the pH of the catalyst solution to pH 9.8 conferred little if any improvement for either catalyst compared with pH 9.0, likely due to background basic hydrolysis of CO_2, as indicated by the significantly greater Y intercept values. Our experiments are consistent with and serve to validate our theoretical predictions that cyclen-Zn^{2+} facilitates faster CO_2 hydration than cyclam-Zn^{2+} at the mild pH conditions optimal for cost-effective industrial CO_2 capture. This feedback between experiment and modeling will help facilitate reliable *in silico* screening of new catalyst candidates for post-combustion CO_2 capture.

Acknowledgement
This work was performed under the auspices of the U.S. Department of Energy by Lawrence Livermore National Laboratory under Contract DE-AC52-07NA27344 with support from Lawrence Livermore National Laboratory (LDRD 10-ERD-035).

[1] Nakata, K.; Shimomura, N.; Shiina, N.; Izumi, M.; Ichikawa, K.; Shiro, M. *Journal of Inorganic Biochemistry* **2002,** 89, 255-266.
[2] Zhang, X.; Eldik, R. v. *Inorganic Chemistry* **1995,** 34, 5606-5614.
[3] Zhang, X.; Eldik, R. v.; Koike, T.; Kimura, E. *Inorganic Chemistry* **1993,** 32, 5749-5755.
[4] Bergquist, C.; Fillebeen, T.; Morlok, M. M.; Parkin, G. *Journal of the American Chemical Society* **2003,** 125, 6189-6199.
[5] Kimura, E.; Shiota, T.; Koike, T.; Shiro, M.; Kodama, M. *Journal of the American Chemical Society* **1990,** 112, 5805-5811.
[6] Kato, M.; Ito, T. *Inorganic Chemistry* **1985,** 24, 504-508.
[7] Norman, P. R. *Inorg. Chim. Acta* **1987,** 130, (1-4).
[8] Shionoya, M.; Kimura, E.; Shiro, M. *Journal of the American Chemical Society* **1993,** 115, (6730-6737).
[9] Khalifah, R. G. *The Journal of Biological Chemistry* **1971,** 246, (8), 2561-2573.